

Absolute Negative Mobility in a Ratchet Flow

Philippe Beltrame¹

UMR1114 EMMAH, Dept. of physics, Université d'Avignon – INRA, F-84914
Avignon, France
(E-mail: philippe.beltrame@univ-avignon.fr)

Abstract. This paper is motivated by the transport of suspended particles pumped periodically through a modulated channel filled of water. The resulting flow behaves as a ratchet potential, called ratchet flow, i.e. the particle may drift to a preferential direction without bias. In order to find out the parameter range of the particle transport and to understand it, we study the deterministic particle dynamics using continuation of periodic orbits and of periodic transport solutions. We identify the onset of transport as a widening crisis. We show that for slightly asymmetric problem, the particle may drift in the opposite direction of the bias. By adding a small noise the onset of transport may be trigger leading to an Absolute Negative Mobility (ANM).

Keywords: Ratchet, Absolute Negative Mobility, synchronization, Chaos, Noise, Continuation.

1 Introduction

The transport of micro-particles through pores in a viscous fluid in absence of mean force gradient finds its motivation in many biological applications as the molecular motor or molecular pump. In the last decade, the literature shows that a periodical pore lattice without the symmetry $x \rightarrow -x$ can lead to the so-called ratchet effect allowing an transport in one direction x or $-x$. A review can be found in Hänggi and Marchesoni[12]. We focus on the setup presented in Matthias and Müller[22] and Mathwig *et al.*[21] consisting in a macroporous silicon wafer which is connected at both ends to basins. The basins and the pore are filled with liquid with suspended particles ($1 - 10\mu m$). The experiment shows the existence of an effective transport in a certain range of parameter values. By tuning them, the direction of the effective transport may change and in particular the transport direction is opposite to the particle weight. These results may be interpreted as a ratchet effect by Kettner *et al.*[14] and Hänggi *et al.*[13] where "ratchet" refers to the noisy transport of particle without bias (zero-bias). When the transport direction is opposite to the bias, then it is called Absolute Negative Mobility (ANM), see e.g. Du and Mei[9] or Spiechowicz *et al.*[27]. Recently, we show that inertia may induce a directed transport Beltrame *et al.*[4]. In this deterministic approach where thermal fluctuations are negligible and a small inertia is taken in to account,



the transport results from non-linear phenomena. Because of the existence of transport without bias, we called the fluid flow in the micro-pump: ratchet flow. Since the results of the experiment of Mathwig *et al.*[21] question the relevance of small fluctuations in the transport, in this paper, we propose to better understand the role of noise in this non-linear dynamics. And especially to focus to a possible Absolute Negative Mobility.

We consider a one-dimensional system where the Stokes force and a small random force due to fluctuations are the only forces acting on the particle. It results a ODE system which is similar to inertia ratchet as found in the literature: Barbi and Salerno[3], Mateos[18,19] and Speer *et al.*[26]. In these latter papers, transport solutions synchronized with the periodic forcing are found for the deterministic case. They show that this dynamics results from a synchronization transition as it occurs for periodically forced oscillator Pitkovsky *et al.*[24]. This regime can be destroyed via a crisis which appears after a period-doubling cascade. The synchronized transport regime may exist in the symmetric case (parity symmetry $x \rightarrow -x$), see Speer *et al.*[26] or Cubero *et al.*[6]. Obviously, it implies the existence of an opposite transport solution and then there is no transport in statistical sense. Now, if a small bias is applied, the domain of existence of opposite transport solutions do not match anymore. As consequence by varying the tuning parameter the transport direction may change and in particular the transport opposed to the bias may exist Wickenbrock *et al.*[30]. The deterministic dynamics may help to understand ANM too. For instance, in Machura *et al.*[16], the nonlinear analysis showed that stable periodic solution and unstable periodic transport solution coexist. By adding a small noise, the trajectory may escape from the bounded periodic solution and may follow during few periods the periodic transport solution. As consequence, a drift opposed to the bias is triggered by the noise.

Despite a plethora of study in this topic, there is still open issues as the transition from unbounded dynamics to transport dynamics which seems no to be clearly identified. Moreover, most of study assumed the inertia large or, in contrary, the limit case of overdamped dynamics (Kettner *et al.*[14] and Lee[15]). Here we consider moderate drag coefficient of the particle. We aim at finding transport transition and possible ANM. In order to tackle this problem we propose to study the deterministic case with inertia particle and then apply a small Gaussian noise. In addition to the time integration, the deterministic case is analyzed with the help of continuation method (Beltrame *et al.*[5] and Dijkstra *et al.*[7]). This method appears seldom in the literature dealing with ratchet (see e.g. Pototsky *et al.*[25]). However, we can follow periodic orbit (or relative periodic orbit for the transport solution) and determine their stability and bifurcation point. Thus, it is powerful to determine onsets and the kind of bifurcation.

In the present work, we consider the physical parameters: particle drag (inverse of the inertia), the mean flow of the fluid, the velocity contrast, the asymmetry of the flow and the bias (resulting from the particle weight). We analyze firstly the bounded periodic solution (symmetric and asymmetric cases), Secondly, the onset of transport is determined. Finally, we treat the case of the small perturbation due to a Gaussian noise.

2 Modeling

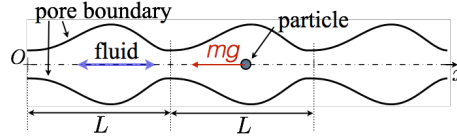


Fig. 1. Sketch of the problem: the particle translates along the x -axis of a periodic distribution of pores. It is dragged by a periodic motion of a viscous fluid. The particle weight is oriented to the negative x direction.

Let us consider a L -periodic varying channel along the line (Ox) (Figure 2) through which a viscous fluid containing suspended particles is periodically pumped. We assume that the period of the pumping period is small enough to consider a creeping flow. Such an assumption is relevant for periodicity for $L \simeq 10\mu m$ and $T \geq 1ms$ (Kettner *et al.*[14]). The particle is centered on the x -axis then the moment of the particle is neglected and the particle does not rotate. This creeping flow exerts a F_d drag force on the particle along the x axis. The set-up is vertical so that the particle weight, F_w , is oriented to the x negative and the buoyancy force, F_b , to the positive direction. Thus the particle position $x(t)$ is governed by the equation

$$m\ddot{x}(t) = F_d + F_w + F_b \quad (1)$$

To simplify, we assume that F_d is approximatively given by the Stokes drag: $F_d = -\gamma(v(x, t) - v_f(x, t))$, where γ is the drag coefficient and v and v_f are the particle velocity and the fluid velocity without particle, respectively. This expression of the drag force requires that the particle is small comparing to the channel radius. Because, it is quasi-static problem, the fluid velocity distribution without particle is proportional to the amplitude pumping so that we may write: $v(x, t) = u_0(x) \sin(2\pi t)$ for a sinusoidal pumping, where $u_0(x)$ depends on the pore profile. We obtain the adimensional governing equation

$$\ddot{x}(t) = \gamma(u_0(x(t)) \sin(2\pi t) - \dot{x}(t)) + g \quad (2)$$

where the length is scaled by the pore length L , the time by the pumping period T and the drag by m/T and $g = (F_w + F_b)/(mL/T^2)$. This equation admits an unique solution C^2 for a given position and velocity (x_i, v_i, t_i) at a time t_i . In particular, two different solutions cannot have at a given time the same position and velocity. Another straightforward result shows that particle acceleration \ddot{x} and its velocity \dot{x} remain bounded.

The velocity profile $u_0(x)$ gets the periodicity of the geometry. If the pore geometry is symmetric, we consider a sinusoidal velocity profile:

$$u_0(x) = u_m(1 + a \cos(2\pi x)) \quad (3)$$

where u_m is the mean velocity and a the velocity contrast. Otherwise for asymmetric geometry, we consider an additional parameter d related to the asymmetry and then the pore profile is given by:

$$\begin{aligned}
u_0(x) = & u_m + au_m \cos\left(\pi \frac{\bar{x}}{\frac{1}{2} + d}\right) 1_{[0; \frac{1}{2} + d]}(\bar{x}) \\
& + au_m \cos\left(\pi \frac{\bar{x} - 1}{\frac{1}{2} - d}\right) 1_{] \frac{1}{2} + d; 1]}(\bar{x})
\end{aligned} \tag{4}$$

d is the algebraic shift which ranges from $-\frac{1}{2}$ to $\frac{1}{2}$, $\bar{x} = x \bmod 1$ and 1_I is the indicator function of the interval I ($1_I(\bar{x}) = 1$ if $\bar{x} \in I$, otherwise $1_I(\bar{x}) = 0$). Examples of the velocity profiles are shown in Figure 2. Note that, it is possible

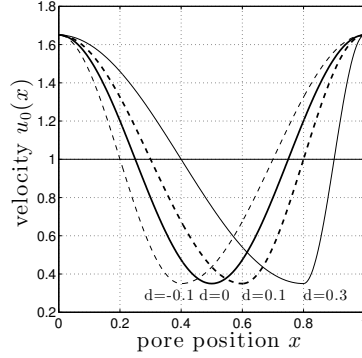


Fig. 2. Analytical velocity profiles of the flow $u_0(x)$ for $u_m = 1$, $a = 0.65$ and different values of d .

to find out pore profiles corresponding to such analytical profiles, see Beltrame *et al.*[4] and Makhoul *et al.*[17]. The asymmetry parameter d does not add a bias: if $g = 0$, the bias remains zero even if $d \neq 0$.

As explained in the introduction, we employ continuation method in order to track the periodic orbits of the Eq. (2) in the parameter space. We use the software AUTO (Doedel *et al.*[8]). This latter requires an autonomous system. In order to obtain an autonomous system and still periodic orbits, we added an oscillator which converges asymptotically to the sinusoidal functions called φ and ϕ :

$$\dot{x} = v \tag{5a}$$

$$\dot{v} = \gamma(u_0(x)\phi - v) + g \tag{5b}$$

$$\dot{\phi} = 2\pi\varphi + \phi(1 - \varphi^2 - \phi^2) \tag{5c}$$

$$\dot{\varphi} = -2\pi\phi + \varphi(1 - \varphi^2 - \phi^2) \tag{5d}$$

where the sinusoidal forcing is the asymptotical stable solution of Eqs. (5c) and (5d), i.e. $\phi \rightarrow \sin 2\pi t$ and $\varphi \rightarrow \cos(2\pi t)$ [2]. The system (5) has the same periodic solution as Eq. (2). This four-dimensional problem can be written

$$\dot{s} = (\dot{x}, \dot{v}, \dot{\varphi}, \dot{\phi}) = F(x, v, \varphi, \phi) = F(s) \tag{6}$$

The deterministic transport is only possible if u_0 is not constant, then the velocity field $u_0(x)$ constitutes the ratchet flow. Considering a symmetric problem, i.e. $u_0(-x) = u_0(x)$ and $g = 0$, the function F is equivariant by the central symmetry $F(-s) = -F(s)$. As consequence, s is solution implies $-s$ is solution too. We called symmetric orbit, solution which are invariant by the central symmetry. There is two symmetric solutions: one centered the pore middle ($x = 1/2$), noted s_m and at the second one, centered at the pore inlet ($x = 0$), noted s_0 .

For the asymmetric case, it is no longer true. However, for small oscillation amplitude u_m , the problem is similar to charged particles in a non-uniform oscillating electromagnetic force McNeil and Thompson[23], it is possible to prove that there exists periodic solution centered at the extrema of $u_0(x)$. At the maximum it is unstable while it is stable at the minimum and it constitutes the only attractor.

Therefore, the analytical results do not show existence of transport solution. In the following we propose to track the periodic solutions in the parameter space.

3 Transitions to transport solutions

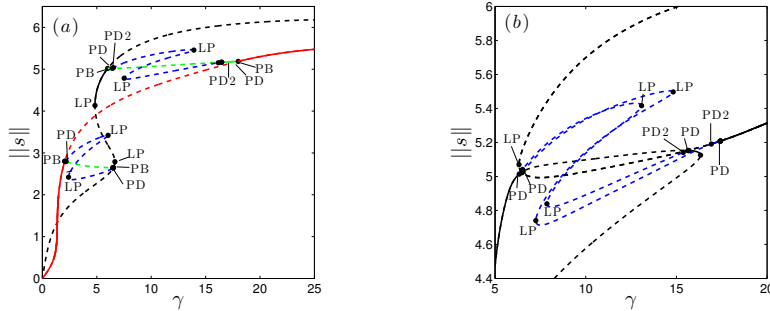


Fig. 3. (a) Bifurcation diagrams showing the periodic branches as a function of the drag γ for $a = 0.65$, $u_m = 9$ in the symmetric case. The black color indicates the s_0 branch, red the s_m branch, green the s_a branch and blue the 2-periodic branch. Dots indicate the different bifurcations: Pitchfork bifurcation (PB), Period-Doubling (PD) and (PD2) for the second period-doubling, fold bifurcation (LP). (b) Bifurcation diagram for the parameter but in the asymmetric case: $d = 0.1$ and $g = -0.1$. Black indicate 1-periodic branch and blue 2-periodic branch. In both diagrams, plain lines indicate stable orbits while dashed line correspond to unstable orbits.

We study the periodic branches for the symmetric case, i.e., the velocity profile u_0 is symmetric ($d = 0$) and there is no bias ($g = 0$). Besides the solutions s_0 and s_m , we find an asymmetric branch (Figure 3(a)). This branch is not invariant by the central symmetry and there is two branches s_a^+ and s_a^- copies by the central symmetry. Then, they have the same norm and they

do not appear in the bifurcation diagram, we note them s_a to simplify. The s_a branch results from a pitchfork bifurcation either from s_0 and s_m and thus connect both branches (Figure 3a). This arises in the intervals $[2.05, 6.52]$ and $[6, 18]$. At each end of the intervals, the same scenario, described below, occurs by varying γ away from the pitchfork bifurcation:

1. The s_a branch is stable in the vicinity of the pitchfork bifurcation but it is destabilized in the via a period doubling. We plotted the bifurcated 2-periodic branch which displays two folds. It becomes unstable via period doubling too. Note that the period-doubling cannot arise on a symmetric branch according to Swift and Wiesenfeld[28].
2. A period doubling cascade follows the first period-doubling and leads to a strange attractor. The present cascade has a behavior similar to one-dimensional map whose the distance between two consecutive bifurcations is divided by the universal Feigenbaum constant [10] $\delta \simeq 4.669$.
3. The strange attractor is bounded till an widening crisis Grebogi et al.[11]. As consequence contiguous attractors (shifted by one spatial period) are connected. Because of the spatial shift symmetry, the dynamics is no longer bounded. Of course for the symmetric case no preferential direction of the particle trajectory is observed. It is more like an anomalous diffusion Mateos and Alatrisme[20].

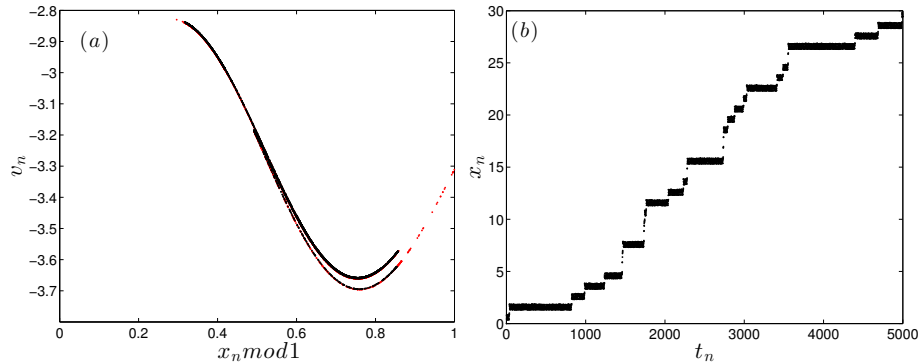


Fig. 4. (a) Poincaré section ($x_n = x(n) \text{ mod } 1, v_n = v(n)$) where $n \in \mathbb{N}$ near the onset of transport at (black dots) $\gamma = 14.70$ and (red dots) $\gamma = 14.69$, other parameters are: $u_m = 9, a = 0.65, d = 0.1, g = -0.1$. The strange attractor in black remains in the interval $[0, 1]$ while the red strange attractor is no longer bounded. Its representation modulo 1 displays a sudden expansion characteristic of the widening crisis. (b) Discrete dynamics $x_n = x(t_n)$ at discrete times $t_n = n$ of the red strange attractor of the panel (a) at $\gamma = 14.69$. An intermittent drift to positive x appears.

For the asymmetric case, similar transitions from 1-periodic orbit to the onset of the transport are observed. Nevertheless, the pitchfork bifurcations of the 1-periodic orbits vanish and instead there is two 1-periodic branches formed,

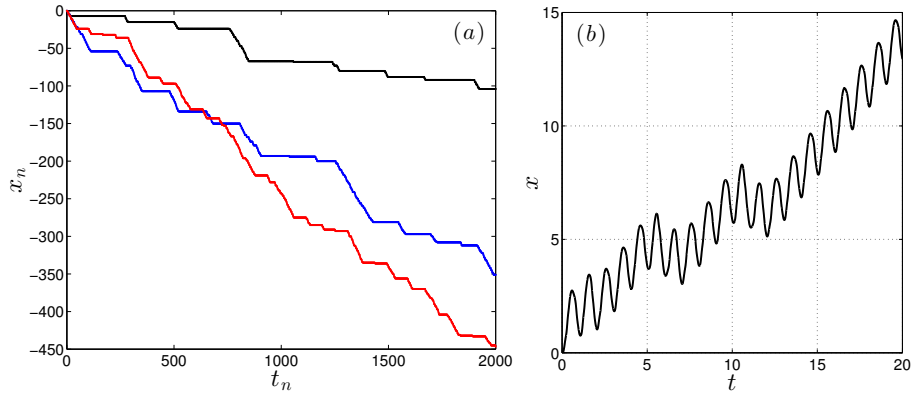


Fig. 5. (a) Discrete dynamics x_n at entire times t_n in the co-moving frame $c = +1$ near the onset of synchronization at (red) $\gamma = 13.4170$, (blue) $\gamma = 13.4165$ and (black) $\gamma = 13.4164 > \gamma_c^s$. Other parameters are $u_m = 9, a = 0.65, d = 0.1, g = -0.1$. The plateaux correspond to a near synchronized transport with $c = +1$. (b) Dynamics $x(t)$ for $\gamma = 13.416 < \gamma_c^s$: After a chaotic transition, the dynamics is the synchronized transport with $c = +1$.

firstly, by the coalescence of the s_0, s_a^+ and s_m and, secondly, by the coalescence of s_0, s_a^- and s_m . An example for $d = 0.1$ and $g = -0.1$ (other parameters being the same as for the symmetric case) is displayed in the bifurcation diagram 3b. From each branch, a period-doubling occurs. Both 2-periodic branches present two folds. A period-doubling cascade arises as for the symmetric case. We focus on the period-doubling cascade which starts at the largest drag coefficient $\gamma \simeq 16.48$. Indeed a drag coefficient smaller than 10 is quite unrealistic for small particles. The period-doubling cascade leads to an asymmetric strange attractor at $\gamma \simeq 15.2$. At $\gamma_c^t \simeq 14.698$, we observe a widening crisis connecting the contiguous attractors (Fig. 4a). But this time, because of the asymmetry of the system, there is a non-zero mean drift particle (see Fig. 4b). As expected, the dynamics after the crisis is intermittent: the dynamics spends a long time near the "ghost" bounded strange attractor and "jumps" to the other "ghost" attractor shifted by one period length. Note that, it is quite unexpected that we obtain a transport opposite to the bias. Now, we study the transport solutions.

4 Transport solutions

By decreasing further the drag coefficient, the drift velocity increases. In fact, the mean duration of the bounded-like dynamics is shorter. For γ approaching the critical value $\gamma_c^s \simeq 13.41639$, the drift velocity is almost equal to one. The epochs of bounded-like dynamics are very short comparing to the transport events. The discrete particle position $x_n = x(t_n)$ at entire times $t_n = n$ and in the comoving frame with the speed $+1$ is displayed in the Fig. 5a. Thus, the long plateaux correspond to the dynamics with drift velocity about one. When γ tends to γ_c^s the longer of the plateaux diverges and then the velocity tends to one. For $\gamma > \gamma_c^s$ the dynamics is periodic in the comoving frame. In other

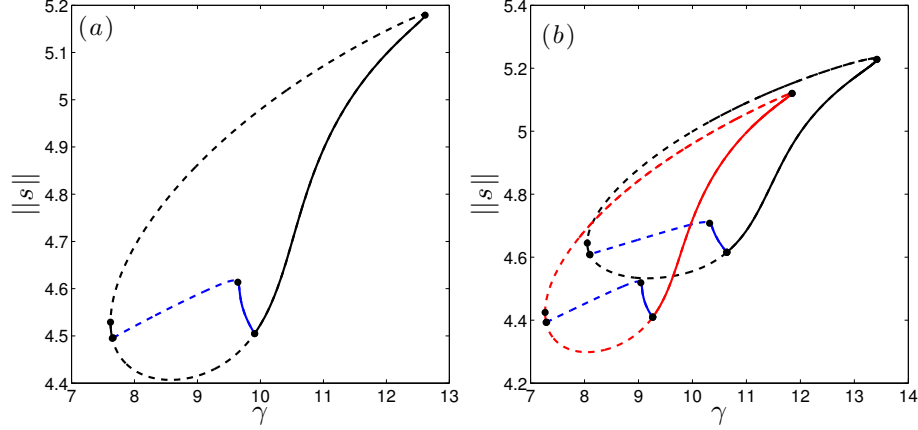


Fig. 6. (a) Bifurcation diagram of the synchronized transport solution with $c = \pm 1$ for the symmetric case. The solution emerges at saddle-node bifurcations. Dashed [plain] line indicate unstable [stable] solution branch. The stable branch becomes unstable via period-doubling (the blue branch corresponds to 2-periodic orbit), which is again unstable by period-doubling. Other parameters are $u_m = 9, a = 0.65$. (b) Bifurcation diagrams of the synchronized transport solution with (red) $c = -1$ and (black) $c = +1$ for the asymmetric case: $d = 0.1, g = -0.1$, the other parameters being the same as in panel (a). A similar bifurcation diagram as for the symmetric case occurs for both branches $c = +1$ and $c = -1$. However, their domains of existence are slightly shifted.

words, the particle advances of one spatial length after one period (Fig. 5b). It is the so-called synchronized transport. In point of view of synchronization, it is a synchronization of oscillators with forcing at moderate amplitude Vincent *et al.*[29]. Then the transition is a saddle-node. Moreover, the chaotic transient observed in Figure 5b suggests the presence of a chaotic repeller as it occurs in this case, see e.g. Pitkovsky *et al.*[24].

We study the regular transport emerging from the synchronization. Since the transport $x_t(t)$ is periodic in the comoving frame, we introduce the periodic function x_p such as

$$x_t(t) = x_p(t) + ct \quad (7)$$

where $c = \pm 1$ depending on the direction of the transport. Then if x_t is solution of Eq. 2 then it is solution of the equation:

$$\ddot{x}_p = \gamma [u_0(x_p + t)) \sin(2\pi t) - \dot{x}_p - c] + g, \quad (8)$$

It is a similar equation as Eq. (2) with an added bias $-\gamma c$. We found a transport with $c = +1$ and also the opposite transport $c = -1$ (Fig. 6b). The coexistence of opposite transport solutions is a consequence of the existence of synchronized transport in the symmetry case. Indeed, for the symmetric case, a similar scenario leads to the synchronized transport (Fig. 6a). In this case, according to the equivariance of the problem, if the solution $c = +1$ is found, then a solution $c = -1$ exists, deduced from the central symmetry (Speer *et al.*[26]). Because these solutions are no more symmetric, generically, these solutions

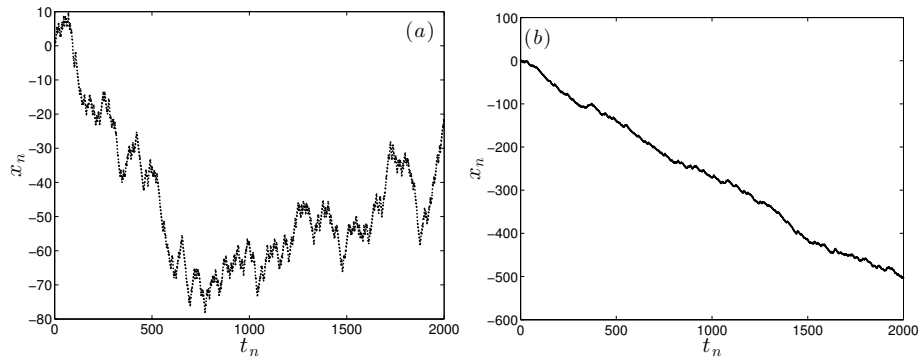


Fig. 7. Discrete time evolutions x_n at entire times t_n for $\gamma = 8.5, u_m = 9, a = 0.65$ and (a) for the symmetric case and (b) the asymmetric case: $d = 0.1, g = -0.1$. The dynamics display a competition between opposite transports. However in the asymmetric case, a net drift to x negative appears.

remain for a small enough perturbation due to the asymmetry d or/and the bias g .

All the bifurcation diagrams of synchronized transport with $c = \pm 1$ have the same structure (Fig. 6). The solution emerges from a saddle-node leading to the birth of a pair of saddle branches. The unstable branch remains unstable over its existence domain. The stable branch becomes unstable via a period doubling bifurcation. As for the bounded periodic solution, a period-doubling cascade occurs leading to a chaotic dynamics. Note however as long as an widening crisis does not occur, the drift velocity remains locked to $c = \pm 1$. After the widening crisis, the strange attractor is no longer bounded in the comoving frame. The resulting dynamics is no longer locked and it is chaotic. Examples for the symmetric and asymmetric cases are displayed in Fig. 7. For the symmetric case, there is a competition between opposite transport solutions which are unstable. The trajectory is unbounded but the mean position remains zero. It is an anomalous diffusion like. For the asymmetric case, the dynamics is similar but the resulting drift is non-zero. For the specific example in Figure 7b, we obtain a net transport direction to the negative direction.

In the asymmetric case, despite the negative bias, there is range where only the upward transport exists ($\gamma \in [11.8457, 13.41639]$). The 'trick' to obtain this unnatural dynamics was, firstly, to introduce the small flow asymmetry d which shifts the existence domains of the transport solutions $c = +1$ and $c = -1$ of the symmetric case (Fig. 6a). Then, this region persists for a small enough negative bias g . Note, without the flow asymmetry d , this region does not exist. In this region, we have a particle motion opposed to the bias like the ANM. To find a upwards dynamics due to the noise, we have to study its influence.

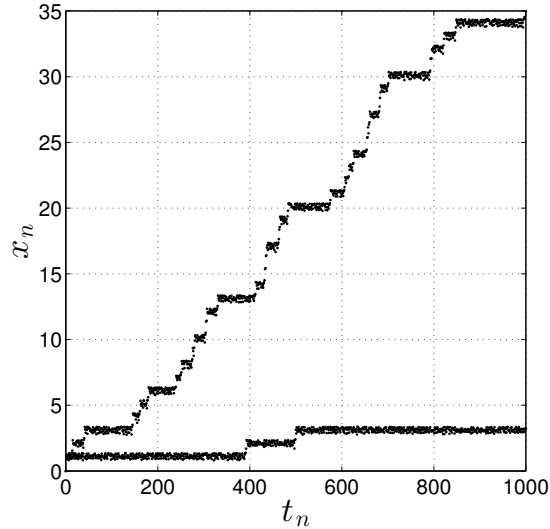


Fig. 8. Discrete stochastic particle dynamics at discrete times n governed by the Eq. (9) with the fluctuation amplitude $\epsilon = 0.1$ for two different values γ near γ_c^t : $\gamma = 14.7$ and $\gamma = 15$ (long plateaux). Other parameters are fixed to $u_m = 9, a = 0.65, d = 0.1, g = -0.1$.

5 Absolute negative mobility

We consider an additional random force, then the ODE system (2) becomes

$$\ddot{x}(t) = \gamma(u_0(x(t)) \sin(2\pi t) - \dot{x}(t)) + g + \epsilon\xi(t) \quad (9)$$

where ϵ is the amplitude of the fluctuating force, and ξ is a Gaussian stochastic process such as $\langle \xi(t) \rangle = 0$ and $\langle \xi(t)\xi(t') \rangle = \delta(t - t')$ where δ is the Dirac delta expressing that the noise is purely Markovian. In contrast to Machura *et al.*[16], the bifurcation diagrams 3 and 6 show that stable bounded periodic solutions do not coexist with unstable transport. Then, it is not possible to obtain the same kind of ANM as in Machura *et al.*[16] where the solution may escape from the stable periodic solution allowing trajectories in the neighborhood of the transport solution leading to the drift emergence. We propose to study the influence of the noise near the onset of unbounded dynamics at the widening crisis. Indeed, before the crisis and in its vicinity, contiguous strange attractors are close together then a small noise may allow to jump from a strange attractor to another one. The simulation near the strange attractor corroborates this scenario (Fig. 8). We observe a dynamics similar to the one which occurs after the crisis. Long epochs of bounded dynamics are interrupted by a jump to the upward pore. We do not observe jump to the downward direction. This is due to the asymmetry of the strange attractor. Note that the simulation in the symmetric case does not display a preferential direction. Away from the crisis by taking larger value of γ , the duration of the bounded dynamics events are statically longer. Indeed it is quite difficult

to distinguish this noisy dynamics from the deterministic dynamics. The noise triggers the crisis transition leading to the same kind of dynamics. Since the transport is opposed to the bias and it does not exist without noise, we have found an example of Absolute Negative Mobility in this framework.

In contrast, once the deterministic crisis occurred, the noise does not notably modified the dynamics and the drift velocity. It seems to have a negligible influence on the onset of the synchronized dynamics too. Moreover, the small noise does not allow to escape from the attraction basin of the periodic transport solution so that it does not destroy the synchronized transport.

6 Conclusion

In this paper we have examined a nonlinear ODE and its perturbation by a small gaussian noise as a model for inertia particle transport via a micro-pump device. The equation is similar to ratchet problem where the ratchet flow $u_0(x)$ variations play the role of the periodical potential in the ratchet literature.

The deterministic analysis showed that synchronized transport solutions exist for inertia particles with drag coefficient about 10. Their existence is not related to asymmetry. Indeed for the symmetric case, the symmetric solution s_0 or s_m becomes unstable via a pitchfork bifurcation. This latter becomes unstable via period-doubling cascade leading to a bounded strange attractor. This strange attractor is destroyed via a widening crisis allowing the emergence of an unbounded dynamics. Finally, via a synchronization transition the periodic transport appears. In the symmetric case, the transports with $c = +1$ and $c = -1$ emerge at the same onset. A similar scenario occurs in the asymmetric case, but the onset of downward and upward transport no longer coincide. When the asymmetry is small, both transport directions exist but their existence domains are shifted. Thus there is a range of the drag coefficient where only the upward transport exists even if the bias is negative.

A weak noise does not modify the synchronized dynamics. However it may trigger the onset of the unbounded dynamics created via an widening crisis. We show that for subcritical parameters, a net drift may appear due to the noise. Indeed, it allows jumps between consecutive bounded strange attractors. We obtain an Absolute Negative Mobility near the onset of the upward transport. This mechanism differs from Machura *et al.*[16] and occurs in a very small range. That shows that the study of the deterministic case and the continuation method is powerful to understand and to find such dynamics. The found ANM is generic of slightly biased ratchet problem. In fact, the scenario involves generic non-linear phenomena: symmetric breaking and crisis in a spatial periodic problem. The existence of an upwards-transport opposed to the bias can be understood as a perturbation of the symmetric case where up and down dynamics coexist. Then for a small perturbation both should exist. Finally, it is quite known that the noise allows to escape from an attractor as it occurs in our case. So, the ANM scenario presented in this paper has a quite universal aspect for ratchet problem.

References

1. Alatrisme, F. R. and Mateos, J. L. (2006). Phase synchronization in tilted deterministic ratchets. *Physica A: Statistical Mechanics and its Applications*, 372(2):263 – 271.
2. Alexander, J. C. and Doedel, E. Jand Othmer, H. G. (1990). On the resonance structure in a forced excitable system. *SIAM J. Appl. Math.*, 50(5):1373171418.
3. Barbi, M. and Salerno, M. (2000). Phase locking effect and current reversals in deterministic underdamped ratchets. *Phys. Rev. E*, 62:1988–1994.
4. Beltrame, P., Makhoul, M., and Joelson, M. Deterministic particle transport in a ratchet flow submitted
5. Beltrame, P., Knobloch, E., Hänggi, P., and Thiele, U. (2011). Rayleigh and depinning instabilities of forced liquid ridges on heterogeneous substrates. *Phys. Rev. E*, 83(1):016305.
6. Cubero, D., Lebedev, V., and Renzoni, F. (2010). Current reversals in a rocking ratchet: Dynamical versus symmetry-breaking mechanisms. *Phys. Rev. E*, 82:041116.
7. Dijkstra, H. A., Wubs, F. W., Cliffe, A. K., Doedel, E., Dragomirescu, I. F., Eckhardt, B., Gelfgat, A. Y., Hazel, A. L., Lucarini, V., Salinger, A. G., Phipps, E. T., Sanchez-Umbria, J., Schuttelaars, H., Tuckerman, L. S., and Thiele, U. (2014). Numerical bifurcation methods and their application to fluid dynamics: Analysis beyond simulation. *Commun. Comput. Phys.*, 15:1–45.
8. Doedel, E., Paffenroth, R., Champneys, A., Fairgrieve, T., Kuznetsov, Y., Sandstede, B., and Wang, X. (2001). Auto 2000: Continuation and bifurcation software for ordinary differential equations (with homcont). Technical report, Caltech.
9. Du, L. and Mei, D. (2012). Absolute negative mobility in a vibrational motor. *Phys. Rev. E*, 85:011148.
10. Feigenbaum, M. J. (1979). The universal metric properties of nonlinear transformations. *J. Statist. Phys.*, 21:669–706.
11. Grebogi, C., Ott, E., Romeiras, F., and Yorke, J. A. (1987). Critical exponents for crisis-induced intermittency *Phys. Rev. A*, 36(11):5365–5380.
12. Hänggi, P. and Marchesoni, F. (2009). Artificial brownian motors: Controlling transport on the nanoscale. *Rev. Mod. Phys.*, 81:387–442.
13. Hänggi, P., Marchesoni, F., and Nori, F. (2005). Brownian motors. In *Ann. Phys.*, volume 14, pages 51–70. Wiley-VCH Verlag.
14. Kettner, C., Reimann, P., Hänggi, P., and Müller, F. (2000). Drift ratchet. *Phys. Rev. E*, 61(1):312–323.
15. Lee, K. (2012). Overdamped transport of particles in a periodic ratchet potential. *Journal of the Korean Physical Society*, 60(11):1845–1850.
16. Machura, L., Kostur, M., Talkner, P., Luczka, J., and Hänggi, P. (2007). Absolute negative mobility induced by thermal equilibrium fluctuations. *Physical Review Letters*, 98(4):040601.
17. Makhoul, M., Beltrame, P., and Joelson, M. (2015b). Particle drag force in a periodic channel: wall effects. In *Topical Problems of Fluid Mechanics : Proceedings, Prague*, pages 141–148.
18. Mateos, J. L. (2000). Chaotic transport and current reversal in deterministic ratchets. *Phys. Rev. Lett.*, 84:258–261.
19. Mateos, J. L. (2002). Current reversals in deterministic ratchets: points and dimers. *Physica D: Nonlinear Phenomena*, 16817169(0):205 – 219. {VII} Latin American Workshop on Nonlinear Phenomena.
20. Mateos, J. L. and Alatrisme, F. R. (2008). Phase synchronization in tilted inertial ratchets as chaotic rotators. *Chaos*, 18:043125.

21. Mathwig, K., Müller, F., and Gösele, U. (2011). Particle transport in asymmetrically modulated pores. *New Journal of Physics*, 13(3):033038.
22. Matthias, S. and Müller, F. (2003). Asymmetric pores in a silicon membrane acting as massively parallel brownian ratchets. *Nature*, 424:53–57.
23. McNeil, B. W. J. and Thompson, N. R. (2010). X-ray free-electron lasers. *Nat Photon*, 4(12):814–821.
24. Pitkovsky, A., Rosenblum, M., and Kurths, J. (2001). *Synchronization. A Universal Concept in Nonlinear Sciences*. Cambridge University Press.
25. Pototsky, A., Archer, A. J., Savel'ev, S. E., Thiele, U., and Marchesoni, F. (2011). Ratcheting of driven attracting colloidal particles: Temporal density oscillations and current multiplicity. *Phys. Rev. E*, 83:061401.
26. Speer, D., Eichhorn, R., and Reimann, P. (2007). Transient chaos induces anomalous transport properties of an underdamped brownian particle. *Phys. Rev. E*, 76:051110.
27. Spiechowicz, J., Hänggi, P., and Luczka, J. (2013). Absolute negative mobility of inertial Brownian particles induced by noise *IEEE 22nd International Conference on Noise and Fluctuations, 24-28 June 2013, Montpellier, France*, 370:446–447.
28. Swift, J. W. and Wiesenfeld, K. (1984). Suppression of period doubling in symmetric systems. *Phys. Rev. Lett.*, 52:705–708.
29. Vincent, U. E., Njah, A. N., Akinlade, O., and Solarin, A. R. T. (2004). Phase synchronization in unidirectionally coupled chaotic ratchets. *Chaos*, 14:1018–1025.
30. Wickenbrock, A., Cubero, D., Wahab, N. A. A., Phoonthong, P., and Renzoni, F. (2011). Current reversals in a rocking ratchet: The frequency domain. *Phys. Rev. E*, 84:021127.